

# How the kinematic swimming of European Eel *Anguilla Anguilla* changes from axial to non-axial velocity flow

Younes Matar, Fabien Candelier, Camille Sollicec

**Abstract**—The aim of this study is to investigate the kinematics of undulatory elongated fish swimming against a velocity flow. We perform the experiments on European eel *Anguilla Anguilla* swimming in a hydrodynamic re-circulating tank with the velocity flow fixed at 0.2 m/s. We find that the undulating shape of overall eel body changes when it swims slantwise from the flow direction, by comparison to axial undulation shape. We examine this kinematics and we propose a general equation describing the lateral position of undulation body taking into account the direction of the eel's swimming.

**Keywords**—undulatory swimming, maneuver, eel *Anguilla Anguilla*, biomechanic.

## I. INTRODUCTION

THIS work is a part of an european project called "ANGELS" consisting on the conception and the construction of a bio-inspired anguilliform robot. We are interested in studying the kinematic behavior of anguilliform swimming fish. Anguilliform swimming is a mode of locomotion in which a travelling undulation is propagated along the body from head to tail [1].

The study of anguilliform swimming has benefited greatly from the attention of such famous scientists as Sir James Gray and Sir James Lighthill. As reviewed by [2], Sir J. Gray [3] has made a pioneer work on undulatory swimming of elongated fish. His work provided the foundation of the groundwork for many subsequent studies on undulatory swimming kinematics. Hence, many kinematics studies were carried out and focused on two extreme behaviors at two ends of the spectrums. At one end of the spectrum, the kinematics of axial undulatory swimming fish are studied [4] - [10] (swimming freely or in parallel to the flow direction). At the other end of the spectrum, very rapid behaviors such as fast start and feeding strikes are studied [11].

The kinematics description of the lateral body displacement during axial undulatory swimming fish has been already accurately described [7]; eel undulates its axial structure symmetrically according to a sinusoidal function with variable amplitude from head to tail. This function reads as:

MATAR Younes (PhD student). Department of Energetic and Environment at Ecole des Mines de Nantes. GEPEA (UMR CNRS 6144). Nantes 44307 France (e-mail: younes.matar@mines-nantes.fr).

CANDELIER Fabien (assistant professor). Aix-Marseille Univ. IUSTI (UMR CNRS 6595). Marseille 13453 France (e-mail: fabien.candelier@univ-amu.fr).

SOLLIEC Camille (professor). Department of Energetic and Environment at Ecole des Mines de Nantes. GEPEA (UMR CNRS 6144). Nantes 44307 France (e-mail: camille.sollicec@mines-nantes.fr).

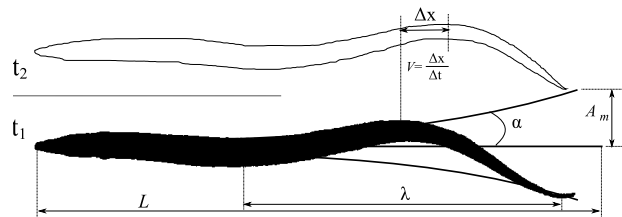


Fig. 1. Sketch of the kinematic parameters of axial undulatory swimming fish

$$y(s, t) = A_m e^{\alpha(\frac{s}{L}-1)} \sin\left(\frac{2\pi}{\lambda}(s - Vt)\right), \quad (1)$$

where  $s$  is the contour length along the body,  $A_m$  the maximum tail beat amplitude,  $\alpha$  the growth amplitude parameter,  $L$  the body length,  $\lambda$  the body wave length,  $t$  the time and  $V$  the body wave speed (see Fig. 1).

To our knowledge, no one has provided a kinematic description of non-axial undulatory swimming, where, fish swims slantwise from the flow direction (fish maintains an angle  $\beta$  with respect to the flow axis).

This study provides the description of the kinematic undulation body of european eel *Anguilla Anguilla*, swimming against to a non-axial velocity flow (slantwise swimming fish). We propose a general equation describing the lateral position of eel body. This equation is based on (1) and takes into account the angle of swimming direction  $\beta$  according to the flow axis.

## II. MATERIALS AND METHODS

### A. Experimental Animals

Our experiments were performed on european eels *Anguilla Anguilla*  $L$  ( $L$  length of eel body). Study was carried out on three individuals with respectively 0.3 m, 0.33 m and 0.38 m body length. One individual was captured on July 2010 (summer) and the others on December 2010 (winter). Eels were returned immediately to the river after achieving the experiments.

### B. Hydrodynamic Test Bench

Experiments were performed in a re-circulating hydrodynamic test bench (see Fig.2). This bench is composed of a large tank (6 m  $\times$  0.8 m  $\times$  1.2 m) separated in two parts by

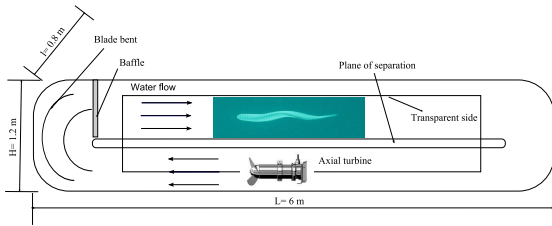


Fig. 2. Sketch of the hydrodynamic test bench with different components

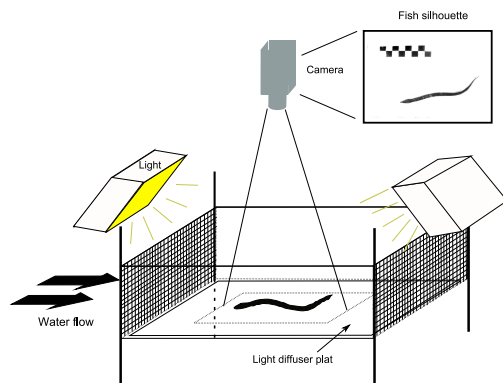


Fig. 3. Experimental procedure; the silhouette of eel was recorded with high speed camera of 60 frames/second

two parallel large plates. A variable-speed axial turbine was used to set the flow velocity in the channel; it could be set up from 0 to 0.5 m/s. Flow velocity was fixed at 0.2 m/s for all experiments. In order to reduce the turbulence of the incoming flow, two bent blades and baffle of flow straighteners were placed at the end of the tank downstream the turbine.

### C. Experimental Procedure

Before the experiment, the animal was allowed to acclimate in the tank by swimming for a few hours in order to discover the new environment. After the acclimating period, we increase step by step the flow speed in order to reach the desired flow velocity.

The eels swam in a fish box (see Fig. 3) with  $1 \text{ m} \times 0.5 \text{ m} \times 0.25 \text{ m}$  working section, immersed of at least 0.15 m from free water surface. To confine eels in the work section, grids with  $0.08 \text{ m} \times 0.08 \text{ m}$  holes covered with a fine mesh were placed upstream and downstream the box (left and right side). We filmed the animal from dorsal view. A light diffuser plate was placed in the bottom of the box. The plat was illuminated by two LED projectors (500 W) placed symmetrically from two sides and inclined  $45^\circ$ . The light system provides a diffused light beneath the swimming animal, therefore, the contrast is increased between eel and camera background.

### D. Kinematics Analysis

Kinematics data were collected only when animals were swimming slantwise and which included at least 2 tail beat cycles. Furthermore, one straight swimming sequence was recorded in order to validate our experimental procedure

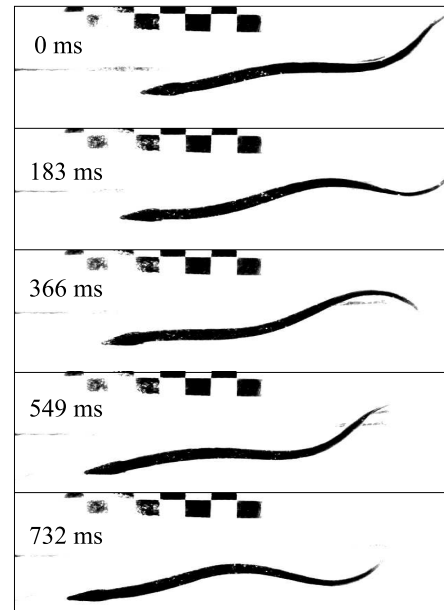


Fig. 4. Sequence of photographs of actual eel swimming in the test bench showing one complete tail beat cycle

and to have a reference for our study. This resulted that 9 sequences for a complete tail beat cycles were retained for analysis. Fig. 4 shows a sequence of photographs from the video recording of a complete tail beat cycle during the eel's slantwise swimming.

Each AVI-sequence was first dissociated to obtain about 22 frames per tail beat cycle. The eel's midlines were obtained via Matlab 7.9 (Mathworks Inc., Natick, MA, USA) as follows: Each grayscale image was converted to a binary image. Then, a specific morphological operation (Skeleton algorithm based on *bwmorph* Matlab function) was applied to the binary image. Finally, the eel's midlines were smoothed, and approximately 350 coordinate pairs per frame were recorded (midline coordinate).

After obtaining the kinematics midlines, the position of the head and the tail was detected manually. The body length was assumed to be equivalent to the number of pixels representing the fish's midline. The average swimming speed was estimated equal to the average of instantaneous swimming speed during one tail beat cycle. The travel's direction was estimated by the average linear regression slope of kinematic midlines from each frame. Fig. 5 shows the kinematic midlines from the eel's slantwise swimming. The solid red line represents the travel's direction which forms an angle  $\beta$  with respect to the flow direction (x axis).

## III. RESULTS AND DISCUSSIONS

When the eel swims freely or against a flow velocity, the body wave amplitude is symmetrically distributed around the axis of motion. Previous works were based on this motion's description to study the kinematic and hydrodynamic of *Anguilliform* swimmer. In our experiments, two modes of forward swimming were observed. In the first case, eels swim in the

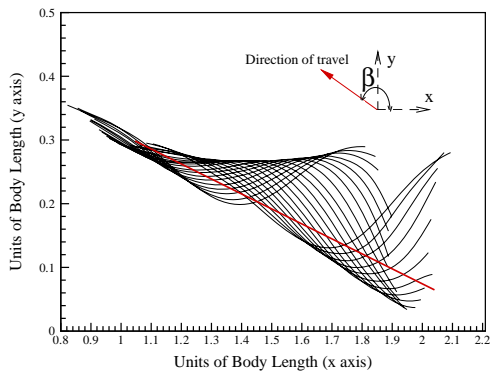


Fig. 5. Kinematic midline (dorsal view) showing a complete tail beat cycle from an eel's slantwise swimming

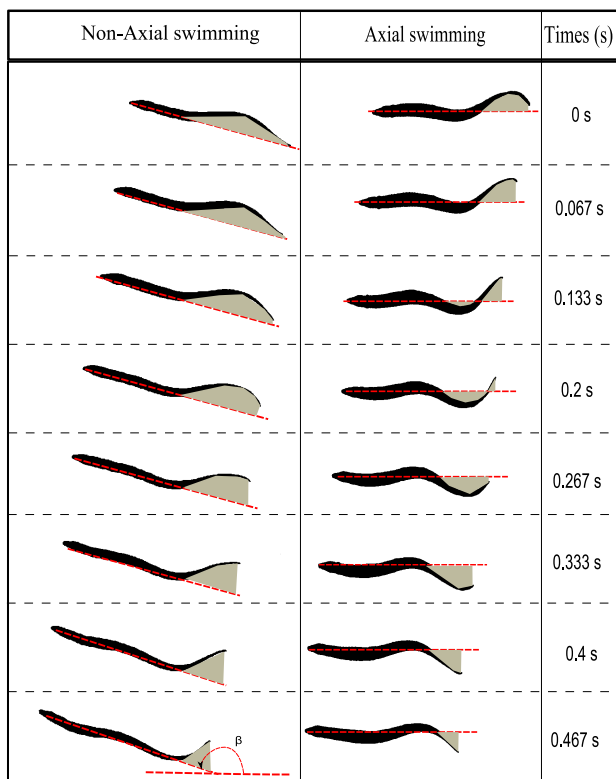


Fig. 6. Silhouettes of the swimming eel over approximately half tail beat cycle. Axial undulatory mode on the right and non-axial mode on the left.

opposite direction of the flow (axial undulatory mode). In the second one, they swim slantwise from the flow direction in order to move forward (non-axial undulatory mode).

In fact, an obvious difference is observed in the amplitude's patterns of these modes. In the second case, the distribution of the body wave amplitude is not symmetric anymore around the axis of motion. This difference can clearly be observed in Fig. 6. It shows silhouettes of the eel's swimming over approximately half tail beat cycle. For axial swimming mode, the maximum and minimum displacements of the tail are reached

TABLE I  
KINEMATIC PARAMETERS FROM REFERENCE [7]

	$U$	$A_m$	$U/V$	$\lambda$	$\alpha$
Min (U)	0.5	0.05	0.57	0.597	3.9
Max (U)	2	0.08	0.797	0.597	2.25

$U$  and  $V$  ( $BL s^{-1}$ ),  $A_m$  and  $\lambda(BL)$

symmetrically from two sides of the red line. However, for non-axial swimming mode, the eel undulates his body mainly from one side of the red line. For that, the difference between these two modes is analysed and represented in the following sections.

#### A. Axial Swimming

To ratify our experimental procedure, especially kinematic analysis, one sequence of an eel's straight swimming is analyzed and compared to previous works. In reference [7], the kinematics of an eel's steadily swimming at speed from  $0.5 BL/s$  to  $2 BL/s$  were quantified in details ( $BL$  is the unit of Body Length). A summary of kinematics swimming parameters is provided in TABLE I.

In our case, eel swims steadily at  $0.87 BL/s$  with maximum amplitude of  $0.077 BL$ . The ratio of swimming speed to body wave speed  $U/V$  is equal to 0.75. The growth amplitude parameter  $\alpha$  is equal to 2.9 and the body wave length  $\lambda$  is equal to  $0.632 BL$ . They are estimated by fitting (1) to the experimental data (nonlinear regression). This result concurs with those represented in TABLE I. The difference in the body wave length is justified because the body wave variation is due to individual variation [7].

Fig. 7 shows the kinematic midlines for a single tail beat sequence where those midlines are superimposed on one another into a body coordinate system. Eel swims in the opposite direction of the velocity flow. The lateral eel body's displacement is represented from: Experimental data Fig. 7(a) and values predicted from the model Fig. 7(b). The accordance between the two graphs allows us to be confident that our experimental procedure and kinematic analysis are reliable.

#### B. Non-Axial Swimming

During experiments, we observed that eel often crosses diagonally the work section to move forwards. They prefer to maneuver when they travel in the opposite direction of an incoming flow. This remarkable behavior is an important feature to be revealed. In fact, this motivates us to interpret the kinematic of non-axial swimming mode. In this mode, eels swim at speed from  $0.58 BL/s$  to  $1.29 BL/s$ . The specific angle of the swimming direction is defined as  $\beta^* = \pi - \beta$ . In fact, since the eel body has a symmetrical shape, the sign of the specific angle does not impact on the swimming kinematic. Thus, the specific angle in these experiments varied, in absolute value, from a minimum of  $8^\circ$  to a maximum of  $26^\circ$ . For example, Fig. 8(a) shows the swimming kinematic midlines (lateral body position) from one complete tail beat

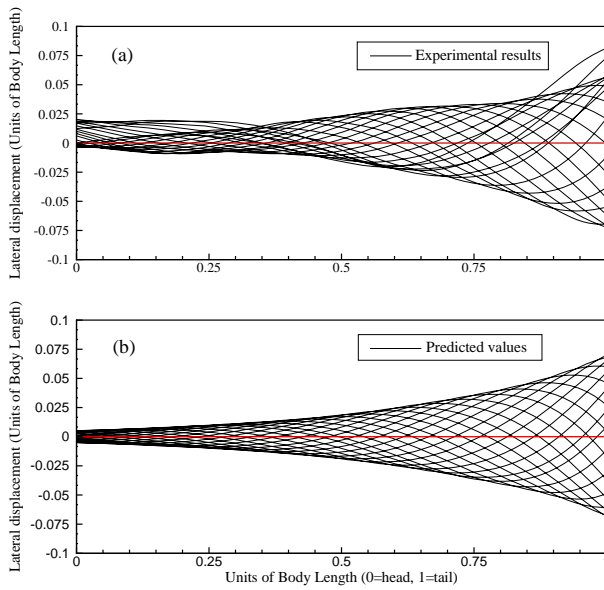


Fig. 7. Lateral displacement of the eel body showing a complete tail beat cycle for axial undulatory swimming eel. (a) Experimental result, (b) values predicted from (1)

TABLE II  
KINEMATIC PARAMETERS

	$V$	$U/V$	$A_m$	$\beta^*$	$\lambda$	$\alpha$	$L$
Axial							
case 1	1.276	0.6842	0.0743	0°	0.632	2.9	0.38
Non-axial							
case 1	1.181	0.6324	0.147	-8°	0.673	2.3	0.3
case 2	1.103	0.7235	0.095	13°	0.697	2.5	0.3
case 3	1.185	0.792	0.094	14°	0.649	2.2	0.33
case 4	1.421	0.6294	0.077	16°	0.612	2.7	0.33
case 5	1.001	0.6509	0.062	17°	0.631	2.8	0.33
case 6	1.081	0.651	0.118	18°	0.697	2.5	0.38
case 7	1.163	0.7229	0.115	-24°	0.706	2.4	0.38
case 8	1.633	0.5829	0.093	26°	0.616	2.1	0.33

$V$  ( $BL s^{-1}$ ),  $A_m$  and  $\lambda$  ( $BL$ ),  $L$  ( $m$ )

cycle with inclination of 13° from the flow direction. Following a coordinates' transform, all midlines are superimposed and rotated until the direction of motion (red line) coincides with the horizontal axis.

After analysing all the swimming sequences, we observed that all kinematics midlines present the same envelope shape of the undulation wave along the fish body. The axis of propagation wave deviates from the swimming direction axis contrary to the axial undulatory mode where the two axis coincide (see Fig. 7). This deviation is more important when  $\beta^*$  increases. In other words, in the axial undulatory swimming mode the inflexion points (i.e. curvature equal to zero) of body curvature follow the swimming direction axis. By contrast,

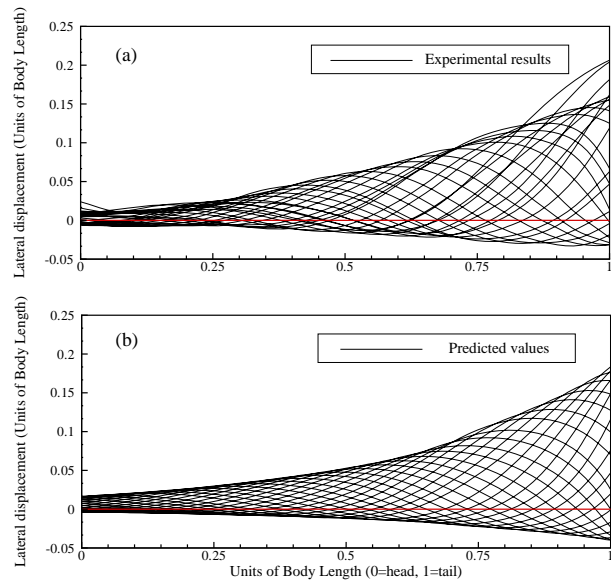


Fig. 8. Lateral eel body's displacement showing a complete tail beat cycle for non-axial undulatory swimming mode ( $\beta^* = 13^\circ$  from the flow axis). (a) Experimental result, (b) values predicted from (2)

in the non-axial undulatory swimming mode, they follow a nonlinear function depending on  $\beta^*$ . This difference notably results from the fact that the interaction between eel body and water flow is more important on the front side than the other side.

Therefore, we propose a general description of the lateral  $y$  position of the midline during forward swimming of the elongated fish. This equation generalizes the description of the lateral body position proposed by [7] by taking into account the specific angle of the fish's swimming  $\beta^*$ . It could be described as:

$$y(s, t) = k A_m e^{\alpha(\frac{s}{L}-1)} \log \left( \sin(|\beta^*|) + e^{\sin(\frac{2\pi}{\lambda}(s-Vt))} \right), \quad (2)$$

where  $k = \beta^*/|\beta^*|$  and the other kinematic parameters are the same as in (1). The kinematic parameters of non-axial undulatory swimming sequences are determined, by fitting (2) to experimental data, and they are given in TABLE II. The kinematic midlines are generated numerically and compared to experimental data in order to validate our model. For example, Fig. 8 illustrates both experimental and numerical midlines corresponding to the case 2 in TABLE II.

Fig. 9 (a) and (b) show a different illustration of the information presented in Fig. 7 and Fig. 8: The lateral oscillation of the different position of the eel's body is presented as a colored curve in function of the times. Each color represents one body coordinate value, selected from the head (dark blue) to the tail (brown) (see the sketch of the Fig. 9(c)). The dotted line represents experimental data and the solid one represents values predicted from the model. We can see that experimental and numerical results are approximately similar in the two cases as confirmed in the sections above.

We can also see that in the axial undulatory mode (i.e. Fig.

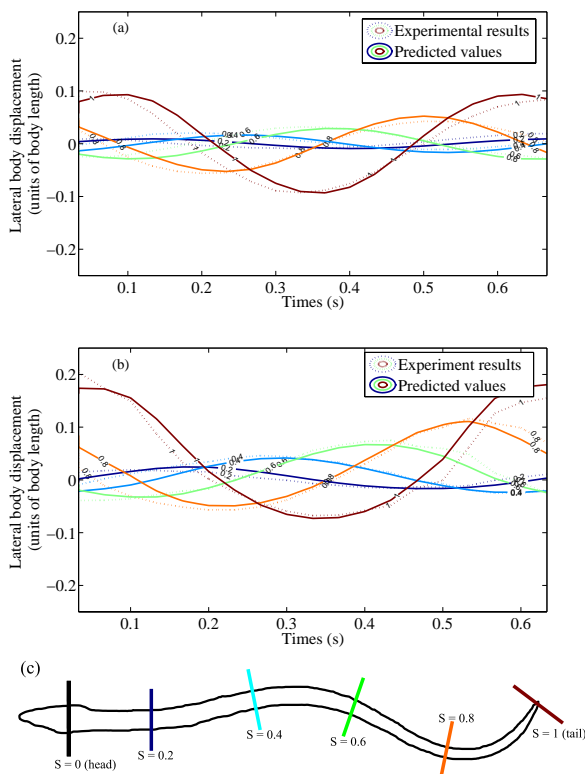


Fig. 9. The lateral oscillation of the different position from the eel's body in function of the time, for axial (a) and non-axial (b) undulatory swimming mode. (c) Sketch showing the different coordinates  $s$  selected from the eel's body. The dotted line represents the experimental data and solid line predicted values

9 (a)), the all part of the eel's body oscillate symmetrically around ( $y=0$ ) the direction of the eel's motion (it can be seen from (1) by considering  $s$  equal to a constant). However, in non-axial undulatory mode (i.e. Fig. 9 (b)), the axis of the oscillation curve deviates from the axis of motion, and this deviation keeps increasing as one goes along the eel's body from the head to the tail (it can be seen from (2) by considering  $s$  equal to a constant). It can be deduced that, when eel swims with a specific angle from the flow direction, it decreases its body's undulation on the front side and benefits from the kinetic energy of the incoming flow to increase its body's undulation on the other side.

#### IV. CONCLUSION

In our experiment we observed two swimming kinematic modes: Axial undulatory swimming mode and non-axial undulatory swimming mode. In the first case, eel swims in the opposit direction of the flow, and in the second one, eel swims slantwise from the direction of the flow. The difference between these modes are studied. we deduce that, when eel swims with an angle from the direction of flow, it decreases its body's undulation on the front side and benefits from the kinetic energy of the incoming flow to increase its body's undulation on the other side. We proposed a general equation

describing the lateral displacement of eel's body by taking into account the direction of swimming. Kinematic midlines are generated numerically and compared to the experimental data in order to validate our model.

#### ACKNOWLEDGMENT

This study was supported by the European Commission, Information Society and Media, Future and Emerging Technologies (FET) contract 231845.

#### REFERENCES

- [1] M. Sfakiotakis and DM Lane and JBC Davies, "Review of fish swimming modes for aquatic locomotion," *IEEE J OCEANIC ENG*, vol. 2, no. 2, pp. 237-252, Apr. 1999.
- [2] GB Gillis, "Undulatory locomotion in elongate aquatic vertebrates: Anguilliform swimming since Sir James Gray," *American Zoologist*, vol. 36, no. 6, pp. 656-665, Dec. 1996.
- [3] J. GRAY, "Studies in Animal Locomotion," *Journal of Experimental Biology*, vol. 10, no. 1, pp. 88-104, Jan. 1933.
- [4] GB. Gillis, "Environmental effects on undulatory locomotion in the American eel *Anguilla rostrata*: Kinematics in water and on land," *Journal of Experimental Biology*, vol. 201, no. 7, pp. 949-961, Apr. 1998.
- [5] K. D'Aout and P. Aerts, "A kinematic comparison of forward and backward swimming in the eel *Anguilla anguilla*," *Journal of Experimental Biology*, vol. 202, no. 11, pp. 656-665, Jun. 1999.
- [6] U. K. Muller and J. Smit and E. J. Stamhuis and J. J. Videler, "How the body contributes to the wake in undulatory fish swimming: Flow fields of a swimming eel (*Anguilla anguilla*)," *Journal of Experimental Biology*, vol. 204, no. 16, pp. 2751-2762, Aug. 2001.
- [7] E. D. Tytell, "The hydrodynamics of eel swimming II. Effect of swimming speed," *Journal of Experimental Biology*, vol. 207, no. 19, pp. 3265-3279, Sep. 2004.
- [8] J. GRAY, "Kinematics and hydrodynamics of linear acceleration in eels, *Anguilla rostrata*," *Proceedings of the Royal Society of London Series B-Biological Sciences*, vol. 271, no. 1557, pp. 2535-2540, Dec. 2004.
- [9] Y. Munk, "Kinematics of swimming garter snakes (*Thamnophis sirtalis*)," *Comparative Biochemistry, Physiology A-Molecular And Integrative Physiology*, vol. 150, no. 2, pp. 131-135, Jun. 2008.
- [10] A. Herrel, Hon-Fai Choi, N. De Schepper, P. Aerts and D. Adriaens, "Kinematics of swimming in two burrowing anguilliform fishes," *Zoology*, vol. 114, no. 2, pp. 78-84, Apr. 2011.
- [11] P. Domenici and R. Blake, "The kinematics and performance of fish fast-start swimming," *Journal of Experimental Biology*, vol. 200, no. 8, pp. 1165-1178, Apr. 1997.